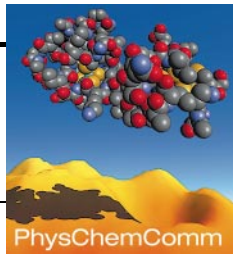

Paper

Glucose induced *in-situ* reduction of chloroaurate ions entrapped in a fatty amine film: formation of gold nanoparticle–lipid composites

Anand Gole, Ashavani Kumar, Sumant Phadtare, A. B. Mandale and Murali Sastry*

Materials Chemistry Division, National Chemical Laboratory, Pune 411 008, India.
E-mail: sastry@ems.ncl.res.in; Fax: +91 20 5893044/5893952; Tel: +91 20 5893044

Received 23rd July 2001, Accepted 20th August 2001
Published on the Web 30th August 2001

The formation of gold nanoparticle–lipid composite films by glucose-induced reduction of chloroaurate ions entrapped in thermally evaporated fatty amine films is described. Simple immersion of films of the salt of octadecylamine and chloroaurate ions (formed by immersion of thermally evaporated fatty amine films in chloroauric acid solution) in glucose solution leads to the facile *in-situ* reduction of the metal ions to form gold nanoparticles in the fatty amine matrix. The formation of gold nanoparticles is readily detected by the appearance of a violet color in the film and thus forms the basis of a possible new, gold nanoparticle-based colorimetric sensor for glucose. The formation of the fatty amine salt of chloroauric acid and the subsequent reduction of the metal ions by glucose has been followed by quartz crystal microgravimetry, Fourier transform infrared spectroscopy, X-ray photoemission spectroscopy and transmission electron microscopy measurements.

1 Introduction

Nanomaterials are expected to play an extremely vital role in many future technologies and this may be attributed to their interesting optoelectronic and physicochemical properties.[1] One aspect of nanotechnology that assumes importance in the context of commercial application of nanoparticles is the organization and packaging of nanoparticles in thin film form. Among the many routes being pursued, the synthesis of nanoparticles (often by the colloidal route) followed by organization on suitable surfaces using principles of self-assembly[2] has received a great deal of attention. Surface modified polymers,[3] terminally functionalised self-assembled monolayers (SAMs)[4,5] and more recently biological templates such as proteins[6] and DNA[7,8] have been used for the organization of nanoparticles in thin films. In a slightly different approach, organized multilayer films of metal salts of fatty acids grown by the Langmuir–Blodgett technique have been used to form quantum dot assemblies by a chemical treatment process.[9,10]

In this laboratory, we have demonstrated that thermally evaporated films of fatty acids when immersed in an aqueous electrolyte solution resulted in the electrostatic entrapment of cations in the lipid film.[11] This process led to the spontaneous self-organization of the fatty acid film into a lamellar, *c*-axis oriented structure similar to that obtained by the conventional LB technique.[11] The use of thermally evaporated ionizable lipid films in the organization of nanoscale entities has since been extended to charged colloidal particles such as silver,[12] gold[13] and CdS quantum dots[14] as well as proteins/enzymes.[15,16] In this report, we extend the methodology based on the extraction of inorganic ions from solution into lipid thin films to the *in-situ* generation of metal nanoparticles. More specifically, we show that $AuCl_4^-$ ions from aqueous solution may be entrapped in thermally evaporated fatty amine films such as octadecylamine (ODA) by simple immersion of the films in electrolyte solution. Thereafter, the aurate ions in the ODA matrix may be reduced *in-situ* by immersion of the $AuCl_4^-$–ODA composite film in glucose solution. This process of reduction of the chloroaurate ions by glucose molecules is seen as the appearance of a dark violet color in the lipid film as the gold nanoparticles are generated (see inset, Fig. 1A). In addition to the realization of gold nanoparticles in thin film assemblies, this procedure may be eventually developed as a gold nanoparticle based colorimetric method for the detection of glucose and draws inspiration from the work of Esumi *et al.*[17] who demonstrated that sugar-persubstituted poly(amidoamine) dendrimers spontaneously reduced chloroaurate ions and led to the formation of gold nanoparticles entrapped in the dendrimers. Presented below are details of the investigation.

2 Experimental

2.1 Chemicals

D-glucose, chloroauric acid and octadecylamine ($CH_3(CH_2)_{17}NH_2$, ODA) were obtained from Aldrich Chemicals and used as-received. Double distilled water was used in all the experiments.

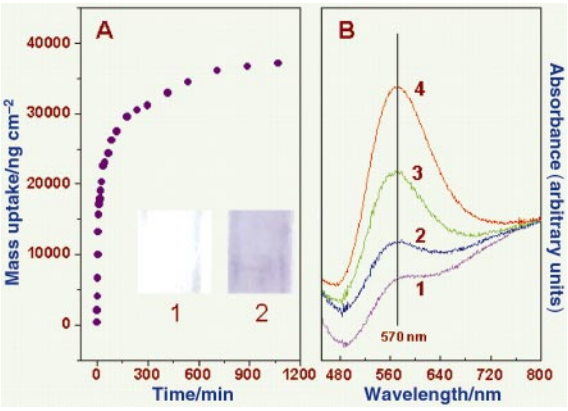

Fig. 1 (A) QCM mass uptake measured as a function of time for a 500 Å thick ODA film during immersion in 10^{-4} M $HAuCl_4$ solution. The inset in this figure shows 2 quartz substrates covered with 500 Å thick ODA films after entrapment of $AuCl_4^-$ ions (1) and after reduction of the $AuCl_4^-$ ions by glucose (2, see text for details). (B) UV-vis spectra of a 500 Å thick $AuCl_4^-$–ODA film on quartz as a function of time of immersion in 0.5 M glucose solution at 60 °C; curves 1–4 are the spectra recorded after 10, 25, 40 and 60 min of immersion, respectively.

2.2 Deposition of ODA thin films

500 Å thick ODA films were deposited on gold coated AT cut quartz crystals (for quartz crystal microgravimetry (QCM) measurements), Si (111) substrates (for Fourier transform infrared spectroscopy (FTIR), X-ray photoemission spectroscopy (XPS) and X-ray diffraction studies (XRD)) and quartz substrates (for UV-vis spectroscopy studies). A 250 Å thick ODA film was also deposited on a carbon-coated transmission electron microscopy (TEM) grid. The deposition of the films was done by thermal evaporation in an Edwards E308A vacuum chamber. The deposition was done at a pressure of 1×10^{-7} Torr and the film deposition rate and thickness were monitored *in-situ* using an Edwards thickness monitor.

2.3 Incorporation of $AuCl_4^-$ ions in ODA films

A 10^{-4} M solution of chloroauric acid was prepared in doubly distilled water. The pH of the chloroaurate ion solution was measured to be 3.5. Chloroaurate ion incorporation into the thermally evaporated ODA films was monitored by immersion of the ODA covered gold coated AT cut quartz crystal for different time intervals in the chloroauric acid solution and measuring the frequency change of the crystal *ex-situ* after thorough washing and drying of the crystal. The frequency counter used was an Edwards FTM5 instrument operating at a frequency stability and resolution of ± 1 Hz. For the 6 MHz crystal used in this investigation, this translates into a mass resolution of 12 ng cm^{-2}. The frequency changes were converted to mass loading using the standard Sauerbrey formula.[18] The time taken for complete ion incorporation determined from the QCM measurements (*ca.* 16 h, see Fig. 1) was used for immersion of ODA coated quartz and Si (111) substrates in the other studies. After thorough rinsing and drying of the $AuCl_4^-$–ODA films, they were further immersed in a 0.5 M glucose solution held at 60 °C for *in-situ* reduction of the chloroaurate ions.

2.4 UV-vis spectroscopy study

500 Å thick $AuCl_4^-$–ODA composite films on quartz substrates were immersed in 0.5 M glucose solution held at room temperature and at 60 °C for different time intervals. UV-vis spectroscopy measurements were carried out on these films using a Shimadzu dual-beam spectrophotometer (model UV-1601 PC) operated at a resolution of 1 nm after thorough washing and drying of the films. A 500 Å thick ODA film on quartz was taken as the reference for UV-vis spectroscopy measurements. For comparison, a 10^{-4} M aqueous solution of $HAuCl_4$ was reacted with 0.5 M glucose held at 60 °C for a period of 2 h and the UV-vis spectrum for this solution was measured.

2.5 Fourier transform infrared spectroscopy (FTIR) measurements

FTIR measurements of a 500 Å thick ODA film on Si (111) substrates before, after chloroaurate ion incorporation and after glucose treatment (immersion in 0.5 M glucose solution held at 60 °C for 2 h) were made on a Shimadzu FTIR-8201 PC instrument operated in the diffuse reflectance mode at a resolution of 4 cm^{-1}. To obtain good signal to noise ratios, at least 256 scans were taken of the composite films in the range 400–4000 cm^{-1}.

2.6 X-ray photoemission spectroscopy (XPS) studies

One 500 Å thick $AuCl_4^-$–ODA composite film on a Si (111) wafer before and after glucose treatment for the period mentioned above was further characterised by XPS measurements. XPS measurements were carried out on a VG MicroTech ESCA 3000 spectrometer equipped with a multichanneltron hemispherical electron energy analyser at a pressure better than 1×10^{-9} Torr. The electrons were excited with un-monochromatized Mg Kα X-rays (energy = 1253.6 eV) and the spectra were collected in the constant analyzer energy mode at a pass energy of 50 eV. This leads to an overall resolution of *ca.* 1 eV for the measurements. The Au 4f, Si 2p (substrate), C 1s and O 1s core level spectra were recorded from the composite films at an electron takeoff angle (ETOA, angle between the surface plane and electron emission direction) of 60°. Prior to curve stripping of the core level spectra by a non-linear least squares procedure, the inelastic electron background was removed by the Shirley algorithm.[19]

2.7 Transmission electron microscopy (TEM) measurements

TEM analysis of a 250 Å thick $AuCl_4^-$–ODA composite film deposited on a TEM grid after immersion in 0.5 M glucose solution (60 °C) for 2 h was performed on a JEOL Model 1200EX instrument operated at an accelerating voltage of 120 kV.

2.8 X-ray diffraction (XRD) studies

A 500 Å thick $AuCl_4^-$–ODA composite film on a Si (111) substrate after immersion in 0.5 M glucose solution held at 60 °C for 2 h was analysed by XRD measurements. These measurements were made on a Philips PW 1830 instrument operating at 40 kV voltage and a current of 30 mA with Cu Kα radiation. The size of the colloidal gold particles in the composite film was estimated from the peak width of the (111) Bragg reflection using the Debye–Scherrer formula.[20]

3 Results and discussion

Fig. 1A shows the QCM mass uptake data measured as a function of time of immersion of a 500 Å thick ODA film in 10^{-4} M $HAuCl_4$ solution. It is observed that there is a large mass increase in the film with equilibration of the $AuCl_4^-$ ion concentration in the ODA matrix occurring after *ca.* 15 h of immersion. The entrapment of the $AuCl_4^-$ ions in the ODA matrix occurs through attractive electrostatic interaction between the gold anions and the protonated amine molecules (please note that the pH of the $HAuCl_4$ solution is 3.5) in the thermally evaporated lipid film. From the equilibrium mass loading of the chloroaurate ions (37 μg cm^{-2}) in this film and a knowledge of the ODA mass deposited initially, an ODA : $AuCl_4^-$ molar ratio of 1 : 5 was calculated. This result clearly indicates an overcompensation of the positive charge in the amine matrix by the gold anions. Such charge overcompensation is known to occur in layer-by-layer electrostatically assembled systems.[21]

From the QCM measurements (Fig. 1A) an optimum time of immersion of the ODA films in $HAuCl_4$ solution of 18 h was chosen. Fig. 1B is a plot of the UV-vis spectra recorded from a 500 Å thick $AuCl_4^-$–ODA film after various times of immersion in 0.5 M glucose solution held at 60 °C. Curves 1–4 correspond to spectra recorded at 10, 25, 40 and 60 min, respectively, after immersion in glucose solution. It is observed that there is a strong absorption band centered around 570 nm in the spectra of Fig. 1B. This band is due to excitation of surface plasmon vibrations in the gold nanoparticles generated in the ODA matrix and gives gold colloids their vivid color.[22] The presence of this resonance in the $AuCl_4^-$–ODA films is therefore a strong indication of *in-situ* reduction of the metal ions leading to the formation of gold nanoparticles. It has been demonstrated that sugar-persubstituted poly(amidoamine) dendrimers reduce chloroaurate ions in solution thereby leading to the formation of gold nanoparticles in solution.[17] Furthermore, it was shown that the hydroxyl groups of the sugar moieties in the dendrimers participated in the reduction

of the metal ions.[17] We believe that a similar mechanism is operative here and that free glucose molecules in solution access the entrapped $AuCl_4^-$ ions present in ODA matrix leading to their *in-situ* reduction.

It is seen from Fig. 1B that there is a monotonic increase in the surface plasmon resonance intensity with time indicating reduction of the entrapped $AuCl_4^-$ ions to yield gold nanoparticles. The intensity of this absorption band stabilizes after this time period and indicates almost complete reduction of the entrapped $AuCl_4^-$ ions in the composite film. For comparison, the UV-vis spectrum recorded from a 10^{-4} M $HAuCl_4$ solution after reduction with 0.5 M glucose (60 °C) for 2 h was recorded (data not shown for brevity). A strong surface plasmon resonance is observed from the solution as well indicating that free glucose molecules in solution may be used to generate gold nanoparticles by reduction of $AuCl_4^-$ ions. It is interesting to note a shift in the surface plasmon resonance wavelength of the gold particles in solution (530 nm) relative to the plasmon resonance wavelength in the film (curves 1–4, 570 nm). This shift is a consequence of the difference in the dielectric properties of the medium surrounding the gold nanoparticles (water and ODA film) and may be easily interpreted in terms of the Mie theory for optical properties of colloidal particles.[13] The rate of reduction of the $AuCl_4^-$ ions in the composite film immersed in glucose solution at room temperature was much slower (data not shown) and required nearly 24 h to achieve an absorbance value equal to that measured for the composite film immersed in the glucose solution held at 60 °C for 1 h.

The highlight of this approach, as mentioned earlier, is the fact that the generation of gold nanoparticles is immediately observable to the naked eye as appearance of a violet coloration in the nano-gold hybrid film. The inset of Fig. 1A shows 2 quartz substrates coated with 500 Å thick thermally evaporated ODA films after immersion in $AuCl_4^-$ solution for 18 h (1) and the $AuCl_4^-$–ODA composite film after immersion in 0.5 M glucose solution at 60 °C for 2 h (2). A violet–blue coloration of the film is clearly observed in the film immersed in glucose solution, which was missing in the $AuCl_4^-$–ODA composite film. We believe that this approach using entrapped $AuCl_4^-$ ions in thermally evaporated ODA films shows promise for development into a 'dip-stick' method for the colorimetric detection of glucose.

The formation of the $AuCl_4^-$–ODA composite film and the *in-situ* reduction of the chloroaurate ions by glucose was followed by FTIR measurements and the spectra obtained in the range 1450–1700 cm^{-1} are shown in Fig. 2A. The spectra labelled 1–3 in Fig. 2A correspond to the 500 Å thick as-deposited ODA film on Si (111) wafer, the ODA film after immersion in 10^{-4} M $HAuCl_4$ solution for 18 h and the $AuCl_4^-$–ODA film after immersion in 0.5 M glucose solution at 60 °C for 2 h, respectively. It is seen that the band at *ca.* 1480 cm^{-1}, which is assigned to the $-NH_3^+$ asymmetric deformation vibrational mode, is clearly present in the as-deposited ODA film (curve 1, feature a) and is considerably reduced in intensity on formation of a complex with $AuCl_4^-$ ions (curve 2). This is a clear indication of the electrostatic complexation of $AuCl_4^-$ ions with the protonated amine molecules in the lipid film and has been observed in Langmuir–Blodgett films of octadecylamine complexed with chloroplatinic acid anions.[23,24] The methylene scissoring band, which occurs at *ca.* 1450 cm^{-1}, is clearly observed in the $AuCl_4^-$–ODA film (curve 2) and appears as a shoulder in the spectrum of the as-deposited ODA film (curve 1).

While not very pronounced, the methylene scissoring band as well as the $-NH_3^+$ asymmetric deformation band can be seen in the $AuCl_4^-$–ODA film after generation of the gold nanoparticles (curve 3). The band at *ca.* 1570 cm^{-1} seen in all the films is assigned to the N–H bend mode of vibration of the protonated amine groups in the ODA matrix.[25]

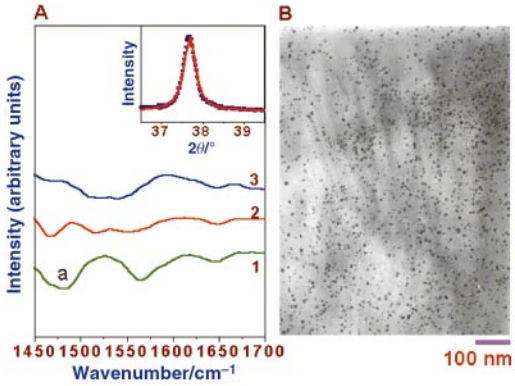

Fig. 2 (A) FTIR spectra recorded from a 500 Å thick as-deposited ODA film on Si (111) wafer (curve 1); the ODA film after incorporation of $AuCl_4^-$ ions (curve 2) and the $AuCl_4^-$–ODA film after reduction of the $AuCl_4^-$ ions by glucose (curve 3, see text for details). The inset shows the XRD pattern recorded from the $AuCl_4^-$–ODA film after reduction of the chloroaurate ions by glucose. The (111) Bragg reflection from the gold nanoparticles is shown along with a Lorentzian fit to the data. (B) TEM micrograph of a 250 Å thick ODA film after incorporation of $AuCl_4^-$ ions and their reduction by glucose; the well dispersed gold nanoparticles are shown.

The TEM picture obtained from a 250 Å thick $AuCl_4^-$–ODA film after immersion in 0.5 M glucose solution held at 60 °C for 2 h is shown in Fig. 2B. The well dispersed gold nanoparticles can clearly be seen in the TEM picture and are uniformly distributed over the film surface. A statistical analysis of 150 gold nanoparticles over the surface of the film was performed and yielded mean particle diameter of 76 Å with a standard deviation of 14 Å. We would like to mention here that regions of highly aggregated gold nanoparticles were also observed in the TEM studies (data not shown) and have been excluded in the particle size analysis. X-ray diffraction was also used to estimate the size of the gold particles formed in the ODA matrix. The inset of Fig. 2A shows the (111) Bragg reflection from gold recorded from a 500 Å thick ODA on Si (111) substrate after formation of the gold nanoparticles. This reflection was fit to a Lorentzian (solid line, inset of Fig. 2A) and the size of the gold nanoparticles was estimated from the line-broadening of the (111) reflection using the Debye–Scherrer formula[20] to be 285 Å. There is a difference in the mean particle size as measured by the TEM (76 Å) and XRD (285 Å) techniques. We believe that the TEM measurements are more sensitive to the particle size distribution whereas XRD gives an overall average of the particle size in the lipid film, which, as mentioned above, showed regions of densely packed gold nanoparticles. Another reason for the difference could be the fact that the film thickness (and consequently the gold loading) was higher for the film subjected to XRD analysis. In any case, the results presented above clearly show that well-dispersed gold nanoparticles can be synthesized by *in-situ* reduction of $AuCl_4^-$ ions entrapped in fatty amine films.

The *in-situ* reduction of entrapped $AuCl_4^-$ ions in the ODA matrix by glucose was followed by XPS measurements. Fig. 3A shows the Au 4f core level from a 500 Å thick ODA after immersion in 10^{-4} M $HAuCl_4$ solution for 18 h. In the XPS measurements, the Au 4f, Si 2p, O 1s and N 1s core level spectra were aligned with respect to the adventitious C 1s binding energy (BE) of 285 eV. The Au 4f spin–orbit components can clearly be seen in Fig. 3A and have been resolved in the figure. The Au $4f_{7/2}$ peak occurs at a BE of 86.4 eV which is considerably higher than that expected for metallic gold (84 eV).[26] The shift to higher BE of the Au $4f_{7/2}$ component clearly shows that Au is in a higher oxidation state commensurate with the +3 oxidation state in the $AuCl_4^-$ anionic complex. The presence of just one component indicates that all the gold atoms in the ODA film are in the same

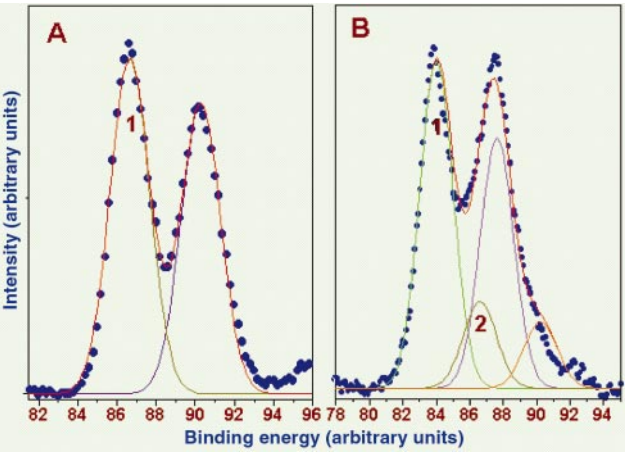

Fig. 3 (A) XPS Au 4f core level spectrum recorded from a 500 Å thick ODA film after incorporation of $AuCl_4^-$ ions. The individual Au $4f_{7/2}$ and $4f_{5/2}$ spin–orbit components are also shown in the figure. (B) XPS Au 4f core level spectrum recorded from a 500 Å thick ODA film after incorporation of $AuCl_4^-$ ions and their reduction with glucose (see text for details). The spectrum has been decomposed into two spin–orbit pairs which are labelled 1 and 2 in the figure. These chemically distinct components are discussed in the text.

oxidation state. The Au 4f core level spectrum recorded after immersion of the $AuCl_4^-$–ODA film in 0.5 M glucose solution held at 60 °C for 2 h is shown in Fig. 3B. The Au 4f core level could now be resolved into two spin–orbit pairs with Au $4f_{7/2}$ BEs of 84 eV and 86.8 eV. The lower BE component arises from metallic gold[26] and provides additional evidence for the generation of gold nanoparticles in the ODA matrix. The higher BE component corresponds to $AuCl_4^-$ ions that were not reduced by the glucose molecules. The ratio of the reduced to un-reduced gold metal ions may be easily calculated from the areas of the peaks marked 1 and 2 in Fig. 3B to be 3.8. While not particularly germane to the process of reduction of the chloroaurate ions by glucose, the N 1s spectrum showed a single component at 399 eV (data not shown) and is due to electron emission from the amine groups of the ODA matrix. The Si 2p and O 1s BEs were commensurate with electron emission from Si and O atoms in SiO_2, the native oxide layer covering the Si wafer.

In conclusion, it has been shown that the reduction of $AuCl_4^-$ ions entrapped within a thermally evaporated fatty amine film by simple immersion in glucose solution leads to the formation of gold nanoparticles in the lipid matrix. This process may be extended to the formation of patterned assembly of nanoparticles using suitable masking procedure during deposition of the lipid film. The *in-situ* reduction of immobilized aurate ions in thin films by glucose is particularly exciting from the point of view of development of a 'dip-stick' method[27] for a gold nanoparticle based colorimetric glucose sensor and is currently being pursued.

Acknowledgements

Two of us, AG and AK, thank the Council of Scientific and Industrial Research (CSIR), Government of India, for financial assistance. The authors thank Dr. Mohan Bhadbade, Materials Chemistry Division, NCL Pune for assistance with TEM measurements.

References

1 See the 28 Feb. 2000 issue of *Chem. Eng. News* and articles by R. Dagani therein for coverage of new applications envisaged for nanomaterials.
2 D. Philip and J. F. Stoddart, *Angew. Chem., Int. Ed. Engl.*, 1996, **35**, 1155.
3 R. G. Freeman, K. C. Grabar, K. J. Allison, R. M. Bright, J. A. Davis, A. P. Guthrie, M. B. Hommer, M. A. Jackson, P. C. Smith, D. G. Walter and M. J. Natan, *Science*, 1995, **267**, 1629.
4 S. Peschel and G. Schmid, *Angew. Chem., Int. Ed. Engl.*, 1995, **34**, 1442.
5 A. Gole, S. R. Sainkar and M. Sastry, *Chem. Mater.*, 2000, **12**, 1234.
6 U. B. Sleytr, P. Messner, D. Pum and M. Sara, *Angew. Chem., Int. Ed.*, 1999, **38**, 1034.
7 J. L. Coffer, *J. Cluster Sci.*, 1997, **8**, 159.
8 M. Sastry, A. Kumar, S. Datar, C. V. Dharmadhikari and K. N. Ganesh, *Appl. Phys. Lett.*, 2001, **78**, 2943.
9 R. S. Urquhart, D. N. Furlong, H. Mansur, F. Grieser, K. Tanaka and Y. Okahata, *Langmuir*, 1994, **10**, 899.
10 Z. Pan, J. Liu, X. Peng, T. Li, Z. Wu and M. Zhu, *Langmuir*, 1996, **12**, 851.
11 P. Ganguly, M. Sastry, S. Pal and M. N. Shashikala, *Langmuir*, 1995, **11**, 1078.
12 M. Sastry, V. Patil and S. R. Sainkar, *J. Phys. Chem. B*, 1998, **102**, 1404.
13 V. Patil, R. B. Malvankar and M. Sastry, *Langmuir*, 1999, **15**, 8197.
14 V. Patil, K. S. Mayya and M. Sastry, *J. Chem. Soc., Faraday Trans.*, 1997, **93**, 4347.
15 A. Gole, C. V. Dash, M. Rao and M. Sastry, *Chem. Commun.*, 2000, 297.
16 A. Gole, C. V. Dash, A. B. Mandale, M. Rao and M. Sastry, *Anal. Chem.*, 2000, **72**, 4301.
17 K. Esumi, T. Hosoya, A. Suzuki and K. Torigoe, *Langmuir*, 2000, **16**, 2978.
18 G. Sauerbrey, *Z. Phys. (Munich)*, 1959, **155**, 206.
19 D. A. Shirley, *Phys. Rev. Sect. B.*, 1972, **5**, 4709.
20 J. W. Jeffrey, *Methods in Crystallography*, Academic Press, New York, 1971.
21 D. Decher, *Science*, 1997, **277**, 1232 and references therein.
22 The vivid pink–violet colors of gold nanoparticles arise due to excitation of surface plasmon vibrations in the nanoparticles that occur in the visible region of the electromagnetic spectrum (S. Underwood and P. Mulvaney, *Langmuir*, 1994, **10**, 3427).
23 S. Pal, PhD Thesis, University of Poona, 1996.
24 G. Ning, Z. Guangfu and X. Shiquan, *J. Mol. Struct.*, 1992, **275**, 85.
25 D. V. Leff, L. Brandt and J. R. Heath, *Langmuir*, 1996, **12**, 4723.
26 C. S. Fadley and D. A. Shirley, *J. Res. Natl. Bur. Stand. (US)*, 1970, **74A**, 543.
27 K. L. Campbell, *Prog. Clin. Biol. Res.*, 1988, **285**, 237.